Inverse problems of nonlinear dynamics of vector class-*A* lasers with anisotropic Kerr-type material

A. Kul'minskii
Institute of Molecular and Atomic Physics, National Academy of Sciences, F. Skarina Avenue 70, 220072 Minsk, Belarus
(Received 18 January 2000; published 17 July 2000)

Nonlinear behavior of weakly anisotropic (vector) lasers with fast material dynamics (class-***A*** lasers) containing an anisotropic Kerr-type nonlinear material inside the cavity has been theoretically explored. Among interesting periodic amplitude-polarization dynamics, such vector nonlinear systems exhibit important features which are promising for progress in the elaboration of simple, inexpensive, and highly sensitive methods of measurement. In particular, it is shown that under stationary laser operation, the turning angle of the polarization plane of the emitted field is a unique measure of the field-independent anisotropy of the Kerr material. In contrast, dynamical features of the system behavior reflect solely influence of the third-order Kerr nonlinearity. As a consequence, the modulus and sign of the coefficient of this nonlinearity can be determined when a linearly polarized laser mode is destabilized at the corresponding Hopf bifurcation point. Accuracy and sensitivity of the measurements in this system can be enhanced by the bistability phenomenon, which is an inherent feature of vector lasers. The dynamics of this system subject to the action of a longitudinal magnetic field is also investigated.

PACS number(s): 42.55.Lt, 42.60.Mi, 42.65.−k, 42.25.Ja

I. INTRODUCTION

Continuing interest in lasers is a consequence of progress in quantum electronics, which leads to the development of new laser devices and new applications that use lasers. Recent achievements in nonlinear dynamics reveal new horizons for laser applications: numerous nonlinear laser systems might be effective tools for solving inverse problems when relevant information about inherent structure of these systems is extracted from the laser output parameters [1]. Furthermore, results of such investigations should be not necessarily limited to laser physics. Indeed, many systems are known to undergo the same nonlinear phenomena irrespective of their specificity. Hence, modeling certain situations in a nonlinear laser system helps to handle realistic cases in other branches of science where these studies would be more time and/or cost consuming. An advantage of lasers is a relatively easy measurement of parameters of the laser field.

However, most of the previous works have emphasized the nonlinear behavior of so-called scalar laser systems. In these systems the emitted laser field is assumed to have certain fixed polarization because of strong anisotropy of either the gain medium (as in the case of solid state or glass lasers, for instance) or the laser cavity (as in the case of a laser with Brewster angle windows). This is not the case for modern commercially available lasers with axially symmetric architecture. The most notable are vertical cavity surface emitting lasers (VCSELs), fiber lasers, microchip lasers, and weakly anisotropic gas lasers with windows placed orthogonally to the resonator axis. The design of these lasers permits the polarization state of the field to evolve almost freely. Thus the polarization (vectorial) degree of freedom can be an essential factor in their dynamics, raising an interesting problem of its impact on progress in the development of inverse methods of extracting information.

On the other hand, it is well known that intense optical (laser) fields may induce field-dependent changes (i.e., intensity and polarization sensitive) in their polarization state during their propagation in a nonlinear medium [2,3]. While these optical nonlinearities are familiar in conventional nonlinear optics, i.e., when the laser field is used as a source for intense light, their effect on the *nonlinear dynamics* of vector lasers containing nonlinear material inside the cavity (in additional to the material of the gain medium) is practically unexplored. Actually, the synthesis of the problem of nonlinear dynamics of vector lasers and the problem of saturable optical anisotropies constitutes a new class of challenging objectives having large potential for applications. It should be also emphasized that this class of problems can be an intrinsic problem for certain lasers, as, for instance, for fiber lasers.

The main goal of this paper is to explore the effect of auxiliary vector optical nonlinearities on the laser dynamics and to show the advantages of this generalized vector problem for further progress in inverse methods of measurements. Because vectorial degree(s) of freedom in lasers considerably complicates their behavior [4], significant progress can be achieved even in the simplest case of a class-*A* [5] vector laser. Recall that corresponding scalar analogs do not exhibit any remarkable dynamics at all [6]. The most familiar and widely used lasers of this type are He-Ne lasers. Moreover, these devices are rather convenient tools for experimentalists since they are readily available, cost effective, and can be easily managed. In this work we study theoretically nonlinear dynamics of such a laser containing a cell filled with anisotropic Kerr-type nonlinear material [2]. We show that a whole complex of stationary and dynamical phenomena exhibited by this system suggests relatively simple, highly sensitive, low cost- and power-consuming methods of measurement of the material anisotropies. It is worth noting that while measurement of the third-order nonlinearities is a rather old problem, it is still of interest because of numerous experimental difficulties extracting desirable information (see Ref. [7] and references therein).

The remainder of this paper is the following. Section II is devoted to the description of the theoretical model. In Sec.

III we discuss the behavior of the laser steady states, the mode stability and time-dependent regimes. The dynamics of this system subject to the action of a longitudinal magnetic field is investigated in Sec. IV. Finally, in Sec. V the main conclusions are summarized.

II. LASER MODEL

Theoretical treatment of the problem is based on the Jones matrix and vector approach, which has been discussed in detail in Refs. [6,8,9]. According to that method, the electric field, considered in the usual plane-wave approximation, is described by the Jones vector **E**

$$\mathbf{E}=\begin{bmatrix} E_{x(+)}e^{i\varphi_{x(+)}} \\ E_{y(-)}e^{i\varphi_{y(-)}} \end{bmatrix} e^{-i\omega t'},$$

where $E_{x,y}$ $(E_{\pm})$ and $\varphi_{x,y}$ $(\varphi_{\pm})$ are the slowly varying amplitudes and phases of the two orthogonal components of the electric field in the Cartesian (circular) basis; ω is frequency of the laser field, and t' is time in seconds. Alternatively, the Jones vector **E** can be expressed in terms of the field intensity $I=\mathbf{E}^h\cdot\mathbf{E}$ ($\mathbf{E}^h$ is the Hermitian conjugate vector of **E**), ellipticity angle β or, equivalently, ellipticity $\xi=\tanh\beta \equiv(E_+-E_-)/(E_++E_-)$, and azimuth of the long axis of the polarization ellipse $\Phi\equiv(\varphi_+-\varphi_-)/2$. In the Cartesian basis it takes the form [8]

$$\mathbf{E}=\sqrt{\frac{I}{\cosh 2\beta}}\begin{bmatrix} \cos(\Phi+i\beta) \\ \sin(\Phi+i\beta) \end{bmatrix} e^{i(\varphi'-\omega t)}. \tag{1}$$

Here $\varphi'\equiv(\varphi_++\varphi_-)/2$ is the mean (global) phase of the electric field, and time t is expressed in round-trip units ($t=t'c/2nL$, where c is the light velocity and nL is the optical length of the laser cavity).

Each anisotropic element inside the cavity, including the gain medium, can be described by a 2×2 Jones matrix. Because these matrices do not necessarily commute, the order of all the anisotropic elements in a laser is significant. To fix the geometry of the problem the following assumptions are done. First, the laser resonator is of a Fabry-Pérot type. Second, the laser gain medium is placed next to the isotropic and fully reflecting mirror. It is worthwhile to note that this is the approximation, which enables an additive contribution of the field-dependent gain medium anisotropy and the anisotropy of the cavity [6], which is a typical situation in the models based on the Lamb approach [10]. Third, a Kerr cell with nonlinear material is placed next to the gain medium. Fourth, an auxiliary linearly (i.e., in the Cartesian basis) anisotropic element is incorporated into the resonator. The role of the latter element is twofold. On the one hand, without this element an effect of the optical anisotropies of the Kerr material in such a laser configuration would disappear. On the other hand, it is quite natural to incorporate such an element since in most cases the cavity optics is not perfect specifically in the Cartesian basis. Furthermore, under certain conditions these numerous anisotropies, which are normally spread throughout the cavity, can be replaced by an effective element with controllable anisotropy [11]. Thus geometry of the setup will be as depicted in Fig. 1.

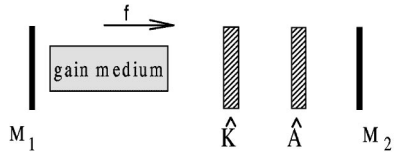

FIG. 1. Scheme for the nonlinear laser system considered in the work. M_1 and M_2 are the mirrors; $\hat{A}$ and $\hat{K}$ are the Jones matrices of the bare laser cavity and the Kerr cell, respectively. The arrow shows the forward direction for the field propagation.

Because the effect of the cavity and the gain medium can be taken into account additively, we can focus on the cavity anisotropy alone. Later, the rate of change of the electric field due to the cavity will be added to the lasing equations. For the laser configuration shown in Fig. 1, the cavity overall matrix, which includes all anisotropies except the nonlinear anisotropy of the gain medium, can be written in the following form:

$$\hat{A}_r=\hat{K}_b\hat{A}_b\hat{A}_f\hat{K}_f=\hat{K}_b\hat{A}\hat{K}_f. \tag{2}$$

Here subscript f (b) refers to forward (backward) matrix. The Jones matrix $\hat{A}$ of the anisotropic element with aligned amplitude and phase anisotropies in the Cartesian basis is

$$\hat{A}=\begin{pmatrix} p_xe^{i\Delta} & 0 \\ 0 & p_ye^{-i\Delta} \end{pmatrix}\equiv\begin{pmatrix} \varepsilon_1 & 0 \\ 0 & \varepsilon_2 \end{pmatrix}, \tag{3}$$

where $p_{x,y}$ are the amplitude transmission factors of the resonator for two orthogonally polarized laser modes, i.e., they are quantities within the range $[0,1]$. Their maximum values, i.e., $p_x=p_y=1$, correspond to the absence of anisotropic absorption in the cavity. Any anisotropy in the x (y) direction reduces p_x (p_y). Parameter Δ is the cavity linear phase anisotropy which is measured in radians (for example, there is no phase anisotropy when $\Delta=0$, whereas $\Delta=\pi/4$ corresponds to a quarter wave plate).

Next, let us determine matrices $\hat{K}_f$ and $\hat{K}_b$. Assuming that the decay rate of the nonlinear polarization of the Kerr material is much larger than the decay rate of the laser field, which can be readily met in class A lasers, overall phase shifts of left $(-)$ and right $(+)$ circularly polarized (CP) components of the laser field in the Kerr cell can be considered to be time independent and expressed as [2,12,13]

$$\phi_{\pm}=\phi_{\pm}^{OA}+\gamma l'\left(\frac{1-B}{2}|E_{\pm}|^2+\frac{1+B}{2}|E_{\mp}|^2\right). \tag{4}$$

Here the first term $(\phi_{\pm}^{OA})$ describes field-independent phase shifts of the CP components of the laser field, which can appear due to the effect of natural optical activity in the Kerr material. The second term provides nonlinear phase accumulations. l' is the length of the Kerr cell, $\gamma=8\pi\omega\chi_{1111}^{(3)}/n_0c$; n_0 is the linear refractive index; $B=\chi_{1221}^{(3)}/\chi_{1111}^{(3)}$; $\chi_{1221}^{(3)}$ and $\chi_{1111}^{(3)}$ are components of the susceptibility tensor of rank 4; $|E_+|^2$ $(|E_-|^2)$ is the intensity of the right (left) CP compo-

nent, which can be expressed in terms of the total field intensity I and ellipticity angle β as

$$|E_{\pm}|^2=\frac{\exp(\pm 2\beta)}{2\cosh 2\beta}I.$$

Then matrices $\hat{K}_f$ and $\hat{K}_b$ in a circular basis read

$$\hat{K}_{f(b)}=\exp\left(\pm i\Delta_+ \pm i\frac{\gamma l' I}{2}\right)\begin{pmatrix}\exp(\pm i\Delta_K) & 0\\ 0 & \exp(\mp i\Delta_K)\end{pmatrix}, \tag{5}$$

where the upper (lower) sign corresponds to the forward (backward) matrix. In Eq. (5) the following notations have been used $\Delta_K=\Delta_- -\gamma l' BI(\tanh 2\beta)/2$ and $2\Delta_{\pm}=\phi_+^{OA}\pm\phi_-^{OA}$.

Substituting expressions (3) and (5), written in the same frame, into expression (2), the cavity Jones matrix in the Cartesian basis takes the form

$$\hat{A}_r=\frac{\varepsilon_1+\varepsilon_2}{2}\hat{I}+\frac{\varepsilon_1-\varepsilon_2}{2}\begin{pmatrix}\cos 2\Delta_K & \sin 2\Delta_K\\ \sin 2\Delta_K & -\cos 2\Delta_K\end{pmatrix}, \tag{6}$$

where $\hat{I}$ is a unit 2×2 matrix. As one can see, the field-independent and nonlinear *isotropic* phase shift $(\Delta_+ +\gamma l' I/2)$ has been explicitly disappeared from the cavity matrix $\hat{A}_r$, which is an advantage of the Fabry-Pérot laser cavity geometry.

To complete with the rate of change of the laser field due to the cavity, we need to know eigenvalues and eigenvectors of matrix (6). It is easily seen that the eigenvalues of $\hat{A}_r$ remain the same as in the case of the absence of the Kerr cell, i.e., they are ε_1 and ε_2. Eigenvectors $\mathbf{E}_{1,2}$ (or, equivalently, $f_{1,2}\equiv\Phi_{1,2}+i\beta_{1,2}$) can be conveniently found using the following formulas [8,14]:

$$\frac{a_{12}+a_{21}}{a_{11}-a_{22}}=-\cot[\Phi_1+\Phi_2+i(\beta_1+\beta_2)], \tag{7}$$

$$\frac{a_{12}-a_{21}}{a_{11}-a_{22}}=-\frac{\cos[\Phi_1-\Phi_2+i(\beta_1-\beta_2)]}{\sin[\Phi_1+\Phi_2+i(\beta_1+\beta_2)]}.$$

Here a_{ij} are the elements of matrix (6). The second expression in Eq. (7) implies that

$$\Phi_1-\Phi_2=\pm\pi/2,\quad \beta_1=\beta_2. \tag{8}$$

Since the parameter Δ_K is real, the first expression in Eq. (7) gives

$$\Phi_2=\pi/2+\Delta_- -\gamma l' BI(\tanh 2\beta)/2,\quad \beta_1=\beta_2=0. \tag{9}$$

Recall that I and β are instantaneous parameters of the laser field. Expressions (8) and (9) explicitly establish that the eigenmodes of the considered laser system are orthogonal and linearly polarized. It is worth noting that the polarization azimuth of the cavity eigenmode Φ_1 (or Φ_2) behaves just as it does when a strong linearly polarized optical field propagates through a Kerr cell placed outside a laser cavity [2,3]. Conditions (8) and (9) allow us to employ the same model as in Ref. [6]. For a laser subject to the action of a longitudinal magnetic field (so-called Zeeman lasers) it is given by Eqs. (30) in [6] (it is not repeated here for the sake of compactness). Properties of the Kerr cell in the equations are simply regarded by the parameter $\Phi'\equiv\Phi-\Phi_2$ of that model.

Actually, the parameter of the third-order nonlinearity is rather small and for many materials it ranges from 10^{-15} to 10^{-13} esu (or from 10^{-23} to 10^{-21} SI) [3,15]. Meanwhile, the average intensity of a cw laser is $I\sim 10^4$ Watt m^{-2} [16] and $|\tanh 2\beta|\leqslant 1$. Hence, our laser model can be simplified by expanding trigonometrical functions containing terms with optical nonlinearity in series and keeping only terms of the first order. The field intensity I must also be properly rescaled

$$-\frac{\gamma l' BI\tanh 2\beta}{\tau_0}=-\frac{4l' B\chi^{(3)}_{1111}}{l\chi^{(3)}_m}J\tanh 2\beta$$
$$=-\frac{4l'\chi^{(3)}_{1221}}{l\chi^{(3)}_m}J\tanh 2\beta\equiv -B_K J\tanh 2\beta,$$

where $B_K=4l'\chi^{(3)}_{1221}(l\chi^{(3)}_m)^{-1}$ is a new nonlinearity parameter, which is proportional to the ratio of the Kerr to gain media third-order nonlinearities; $\chi^{(3)}_m=\sqrt{\pi}N_m|d_{12}|^4/9\hbar^3 Ku\gamma_1\gamma_2$; $Ku=\Delta\omega_D/(2\sqrt{\ln 2})$; $\Delta\omega_D$ is the width of the Doppler profile at half-amplitude; $N_m=N_2-N_1$ is the difference between the populations of the upper (2) and lower (1) levels in the absence of lasing and spontaneous emission from the level 2 to the level 1; $\hbar$ is the Plank constant; $|d_{12}|$ is the normalized matrix element of the electric dipole moment of the lasing transition; γ_1 and γ_2 are the population decay rates of the levels 1 and 2, respectively; l is the gain medium length; and $J=2I|d_{12}|^2/3\hbar\gamma_1\gamma_2$ is rescaled intensity of the laser field.

Finally, the master lasing equations become

$$\dot{J}=4J\{P-JP_0\mathrm{Re}(M_-\tanh 2\beta+M_+)+\tanh 2\beta\,\mathrm{Re}\,\Delta\overline{W}\}/P_0$$
$$-2\gamma_P J\{(1-\cos 2\Phi''/\cosh 2\beta)/\tau_0$$
$$+B_K J\tanh 2\beta\sin 2\Phi''/\cosh 2\beta\},$$

$$\dot{\beta}=-\{\gamma_P\cos 2\Phi''\sinh 2\beta+\omega_P\sin 2\Phi''\cosh 2\beta\}/\tau_0$$
$$-2J\,\mathrm{Re}\,M_-+2(\mathrm{Re}\,\Delta\overline{W})/P_0+B_K\{\gamma_P\sin 2\Phi''\sinh 2\beta$$
$$-\omega_P\cos 2\Phi''\cosh 2\beta\}J\tanh 2\beta, \tag{10}$$

$$\dot{\Phi}=-\{\gamma_P\sin 2\Phi''\cosh 2\beta-\omega_P\cos 2\Phi''\sinh 2\beta\}/\tau_0$$
$$+2J\,\mathrm{Im}\,M_--2(\mathrm{Im}\,\Delta\overline{W})/P_0-B_K\{\gamma_P\cos 2\Phi''\cosh 2\beta$$
$$+\omega_P\sin 2\Phi''\sinh 2\beta\}J\tanh 2\beta.$$

Here the overdot means a derivative with respect to rescaled time $\tau\equiv t\tau_0$; $\Phi''\equiv\Phi-\Delta_-$; $P=U-\eta^{-1}$; U is a real part of the complex error function which governs the laser gain; η^{-1} denotes isotropic losses; $\gamma_P+i\omega_P\equiv 1/2-\varepsilon_2/2\varepsilon_1$; $M_{\pm}$

$=\{\overline{F}_+ e^{-2\beta} \pm \overline{F}_- e^{2\beta} + (S_A \pm S_B)e^{2\beta} + (S_C \pm S_D)e^{-2\beta}\}/\cosh 2\beta$. Note, parameters $S_A \equiv \overline{D}_{+a} + \overline{G}_{+a}$; $S_B \equiv \overline{D}_{-b} + \overline{G}_{-b}$; $S_C \equiv \overline{D}_{+b} + \overline{G}_{+b}$; $S_D \equiv \overline{D}_{-a} + \overline{G}_{-a}$ and $\overline{F}_\pm$ are independent of the laser field amplitude-polarization parameters

$$\overline{D}_{\pm a} = \alpha_\pm \frac{\mathcal{L}_+}{\Gamma}, \quad \overline{D}_{\pm b} = \alpha_\pm \frac{\mathcal{L}_- + \mathcal{L}^{(2)}(\mp 2\Delta_B')}{\Gamma \mp i\Delta_B},$$

$$\overline{G}_{\pm a} = \alpha_\pm \frac{\mathcal{L}_+}{\Gamma + i\delta_\mp}, \quad \overline{G}_{\pm b} = \alpha_\pm \frac{\mathcal{L}_-}{\Gamma + i\delta_\mp},$$

$$\overline{F}_\pm = \alpha_\pm \frac{\mathcal{L}^{(2)}(\mp 2\Delta_B')}{\Gamma + i\delta_\mp}, \quad \alpha_\pm = \frac{9}{4}\exp\left\{-\left(\frac{\delta_\mp}{Ku}\right)^2\right\}.$$

Here $\delta_\pm = \delta \pm \Delta_B'$; $\delta = \omega - \omega_0$ is the atomic detuning; ω_0 is the frequency of the center of the gain profile; $\Delta_B' = g_L \mu_B B$; g_L is the Landé factor, μ_B is the Bohr magneton, B is the magnetic-field strength; 2Γ is the homogeneous profile width; $\mathcal{L}_\pm = \mathcal{L}^{(0)}/3 \pm \mathcal{L}^{(1)}/2 + \mathcal{L}^{(2)}/6$ and $\mathcal{L}^{(k)}(x) = \Sigma_{n=1,2} L_n(k)(\gamma_n^{(k)} + ix)^{-1} - L_3(k)(\gamma_1^{(k)} + ix)^{-1}(\gamma_2^{(k)} + ix)^{-1}$. The angular-momentum functions $L_n(k)$ are expressed in term of the $6j$ Wigner's symbols [9]; k denotes the tensorial orders, which are scalar ($k=0$), vector ($k=1$), and tensor ($k=2$). Scalar, vector, and tensorial parameters in the laser are the total population of upper and lower manifolds, and the atomic magnetic dipole and electric quadrupole, respectively. $\gamma_{1,2}^{(k)}$ are the corresponding decay rates. In the following we will assume that $\gamma_{1,2} \equiv \gamma_{1,2}^{(0)} = \gamma_{1,2}^{(1)} = \gamma_{1,2}^{(2)}$. Explicit expressions for other parameters used in Eq. (10) are given in Refs. [6,9].

III. STEADY STATES AND DYNAMICS OF THE LASER SYSTEM WITH NO MAGNETIC FIELD

To get insight into the physics of nonlinear phenomena exhibited by the system, in this section we assume that the magnetic field is absent. Mathematically this means that $\Delta\overline{W}$ in Eq. (10) is zero. Self- (M_+) and cross- (M_-) saturation coefficients for this case considerably simplify [6]

$$M_+ \equiv RC_1 = 3(\gamma_1 + \gamma_2)R\exp\{-\delta_{Ku}^2\}\{L_1(0) + 2L_1(2)\}/\Gamma, \tag{11}$$

$$M_- \equiv RC_2 \tanh 2\beta = 9\tanh 2\beta(\gamma_1 + \gamma_2)R\exp\{-\delta_{Ku}^2\} \times \{L_1(1) - L_1(2)\}/2\Gamma.$$

Here $R \equiv R_r + iR_m = 1 + (1 - i\delta/\Gamma)/(1 + \delta^2/\Gamma^2)$, R_r and R_m are real, and $\delta_{Ku} = \delta/Ku$.

Lasing equations in the absence of the magnetic field admit both elliptically polarized (EP) and linearly polarized (LP) solutions. Due to the fact that the EP solutions exist in a very narrow domain of phase space [6,17] which, in addition, is hardly accessible experimentally, we will not focus on them.

The LP solutions of the problem are

$$J_x = P/P_0 R_r C_1, \quad \beta_x = 0, \quad \Phi_x - \Delta_- = 0,$$

$$J_y = (P/P_0 - \gamma_P/\tau_0)/R_r C_1, \quad \beta_y = 0, \quad \Phi_y - \Delta_- = \pm\pi/2. \tag{12}$$

The first conclusion is that the presence of the term Δ_- in Eq. (12) is the only difference of these solutions with respect to the LP states of the laser with no Kerr cell.

Similar to the problem of a bare weakly anisotropic laser, the linear stability analysis of the LP solutions (12) reveals that the full set of linearized equations (or the corresponding Jacobian matrix) can be separated into two subsets. The first subset, which represents the scalar degree of freedom, leads to a single real intensity eigenvalue λ_1 for each of the two LP states

$$\lambda_1^x = -4P/P_0, \tag{13}$$

$$\lambda_1^y = -4(P/P_0 - \gamma_P/\tau_0).$$

These eigenvalues are associated with ordinary behavior of the laser field in many scalar class A lasers. They determine the stability of the x- and y- laser modes with respect to the perturbation of the mode intensity. In other words, they define first laser threshold, i.e., onset of the laser emission, when the laser gain becomes larger than the cavity losses. Asymmetry in expressions (13) is owing to the fact that the x mode is considered to be always tuned to the resonance while the frequency of the y mode has an offset proportional to the cavity anisotropy offset.

The second subset characterizes the vectorial degree of freedom and provides a pair of polarization eigenvalues $\lambda_{2,3}$

$$\lambda_{2,3}^x = [-2\gamma_P - 2J_x' R_r C_2 - \omega_P J_x' B_K \pm \sqrt{\omega_{Px}' + \omega_P J_x' B_K(\omega_P J_x' B_K + 4J_x' R_r C_2 + 4\gamma_P)}]/\tau_0, \tag{14}$$

$$\lambda_{2,3}^y = [+2\gamma_P - 2J_y' R_r C_2 + \omega_P J_y' B_K \pm \sqrt{\omega_{Py}' + \omega_P J_y' B_K(\omega_P J_y' B_K - 4J_y' R_r C_2 + 4\gamma_P)}]/\tau_0.$$

Here $\omega_{Px(y)}' = 4J_{x(y)}'^2 R_r^2 C_2^2 - 4\omega_P^2 \mp 8\omega_P J_{x(y)}' R_m C_2$ is the saturated frequency of the polarization relaxation oscillations for the x- (y-) mode in a laser with no Kerr cell; the upper (lower) sign in $\omega_{Px(y)}'$ denotes the x (y) mode; $J_{x(y)}' \equiv \tau_0 J_{x(y)}$.

It can be seen that in agreement with Eq. (9), amplitude-polarization parameters of the emitted LP laser field do not depend on the strength of the Kerr nonlinearity. Furthermore, neither the intensity nor the ellipticity of this field is affected by the field-independent anisotropy (Δ_-) of the Kerr cell. Unlike this fact, polarization azimuth depends linearly on Δ_-. This azimuth behavior is similar to that found in conventional experiments in nonlinear optics [2,3]. However, an impressive feature of synthesis of the problems of vector lasers and vector nonlinearities lies in the fact that these nonlinearities do affect the *stability* of the LP laser modes. Thus, it can be said that such a vector laser system sets apart contributions of the field-independent anisotropy Δ_- and nonlinear Kerr anisotropy naturally, without any further compli-

cation of the experimental setup. Consequently, this phenomenon can be employed for measurements of these optical anisotropies that will be discussed at the end of this section.

Equations (14) admit both pitchfork and Hopf bifurcations. However, expressions for the pitchfork bifurcations of the x and y modes do not contain the nonlinearity parameter B_K and, in effect, they are precisely the same as for a laser with no Kerr cell. Since their analysis can be found in Ref. [6], we will not concentrate on them.

In contrast, the Hopf bifurcations do depend on B_K. They are subject to the following conditions for the x and y modes, respectively:

$$2\gamma_P + 2J_x' R_r C_2 + \omega_P B_K J_x' = 0, \tag{15}$$

$$2\gamma_P - 2J_y' R_r C_2 + \omega_P B_K J_y' = 0.$$

With no Kerr nonlinearity ($B_K = 0$), Eqs. (15) recover the results of Ref. [6], giving no possibility of Hopf instabilities for the x mode when $C_2 > 0$ ($j \to j'+1$ lasers). In fact, our problem can be even naturally restricted assuming that C_2 is positive because this is the case for most of the commercially available He-Ne lasers. When $B_K \neq 0$ the first expression in Eq. (15) is no longer strictly positive. Hence both of them can cross zero defining instability thresholds for both modes

$$B_K^x = -2(\gamma_P + J_x' R_r |C_2|)/\omega_P J_x', \tag{16}$$

$$B_K^y = -2(\gamma_P - J_y' R_r |C_2|)/\omega_P J_y'.$$

Careful inspection of the expression for B_K^x reveals that the x mode can be destabilized only for certain B_K for which $\sin 2\Delta$ is not complex. The minimum value of this parameter when $\sin 2\Delta$ is still real is

$$B_{Kx}^{\min} = \pm 2\sqrt{1 - p^2 + 4J_x'^2 R_r^2 C_2^2 + 4J_x' R_r |C_2|}/J_x' p, \tag{17}$$

where the parameter characterizing the amplitude anisotropy has been denoted as $p \equiv p_y/p_x$.

For numerical illustration this problem must be quantitatively specified. For the sake of definiteness, a $j=1 \to j'=2$ He-Ne laser operating at $\lambda = 1.15$ μm will be considered. This laser transition is characterized by the angular-momentum functions $L_1(0) = \frac{1}{15}$, $L_1(1) = \frac{1}{20}$, and $L_1(2) = \frac{7}{300}$. Other parameters of this laser are taken from [18]: $Ku = 480$ MHz, $\Gamma = 95$ MHz, $\gamma_1 = 49.92$ MHz, and $\gamma_2 = 45.12$ MHz. The key free parameters for numerical calculations in this work will be the phase anisotropy Δ, the parameter of the amplitude anisotropy p, detuning δ, and laser isotropic losses η^{-1}. These are the parameters that can be readily controllable experimentally. Since the expressions (16) and (17) remain unchanged when Δ (ω_P) and B_K change their sign simultaneously, only negative parameters of the phase anisotropy will be explored in this section. All results for positive Δ (ω_P) can be simply obtained by changing the sign of B_K to the opposite sign.

In Fig. 2 the Hopf instability boundaries for the x and y modes of the tuned to the resonance ($\delta = 0$) laser are represented in the (η, B_K) and (Δ, B_K) planes. The curves in Fig. 2(a) are plotted for several values of Δ given in the figure and fixed amplitude anisotropy ($p = 0.998$). In Fig. 2(b) parameter η was kept fixed at $\eta = 1.33$ while several curves are depicted for different values of p (also given in the figure). In both these figures the x (y) mode is stable ''below'' (''above'') continuous (dashed) curves.

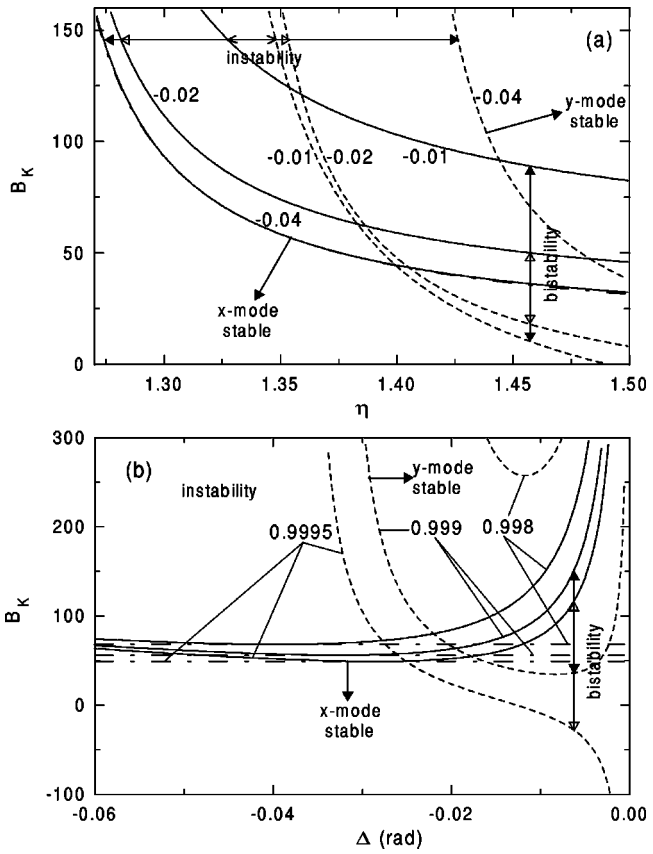

FIG. 2. The Hopf bifurcation points of the LP x (continuous lines) and y (dashed lines) modes and the values of $B_{Kx}^{\min}$ (dashed-dotted lines) are shown in the subspaces (η, B_K) (a) and (Δ, B_K) (b) for different magnitudes of the phase (a) and the amplitude (b) anisotropy (given in the figure). Other free parameters are fixed at $\delta = 0$ and $p = 0.998$ (a) and $\eta = 1.33$ (b). The remaining parameters are the same as those adopted in Sec. III. Note, the dashed-dotted curve in (a) is barely perceptible. The x (y) LP laser mode is stable ''below'' (''above'') the corresponding continuous (dashed) curves. The bistability and the instability domains are pointed by arrows with two arrowheads.

Figure 2(a) shows that bifurcation values of B_K rapidly increase for both modes as the laser net gain decreases, or, equivalently, the losses (η^{-1}) increase. This can be easily understood because for lower intensity the Kerr nonlinearity becomes weaker. Dependence of B_K^x and B_K^y on the anisotropies Δ and p is not so simple [Fig. 2(b)]. In the limit of small amplitude and phase anisotropy, the dominant factor in determining the critical value of B_K is the denominator in Eq. (16). This explains the rapid grows of $B_K^{x,y}$ when Δ approaches zero. Physically this occurs because of progressive compensation of the optical effects in the Kerr cell due to Fabry-Pérot geometry of the laser system when the anisot-

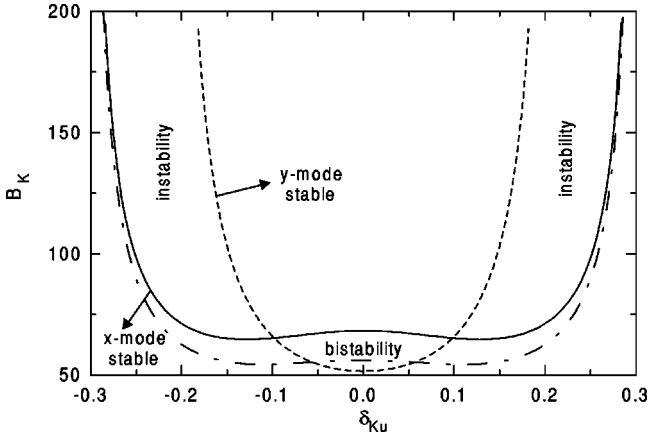

FIG. 3. The same as in Fig. 2 but in the subspace (δ_{Ku}, B_K). The free parameters are fixed at $\eta=1.33$; $\Delta=-0.017$ rad and $p=0.999$.

ropy of the cavity amplitude-phase plate goes to zero (Fig. 1). Increasing the amplitude anisotropy (i.e., decreasing p) makes the change of B_K^x and B_K^y to be smoother for small $|\Delta|$. A qualitative change in the behavior of B_K^y for small amplitude anisotropy [for $p=0.9995$ in Fig. 2(b)] is owing to an interplay among the cavity linear (γ_P) and gain medium nonlinear ($2J_x' R_r C_2$) anisotropies which enter in the stability criteria (15) with opposite signs. Thus, small cavity phase anisotropy is an unfavorable factor for the appearance of instabilities. Increasing $|\Delta|$, the sensitivity of the laser system to the Kerr nonlinearity increases. However, relatively large $|\Delta|$ again gives rise to progressively increasing the instability threshold due to the dominant role of the polarization decay rate γ_P ($\gamma_P \gg R_r C_2$, ω_P) for large $|\Delta|$, although, this growth is not as sharp as in the case when $|\Delta|$ is small. Figure 2(b) displays that the x mode has a larger domain in which it takes minimal values of B_K than the y mode. This follows from our definition that the cavity losses are always larger for the y mode. As is expected, the instability threshold for the x mode increases as the amplitude anisotropy increases.

The detuning dependence of B_K^x and B_K^y again exhibits a drastic reduction in the sensitivity of the laser system to the Kerr nonlinearity at critical values of the control parameter, i.e., at the line edges. A representative example of this dependence is depicted in Fig. 3. Rapid growth of B_K^y as detuning increases, seen in the figure, is due to two factors: (i) the first laser threshold for the y mode is larger than that for the x mode [see (13)] and (ii) the gain medium nonlinear anisotropy interferes destructively (increasing B_K^y) with the Kerr nonlinearity. The curve of B_K^x is rather flat for small and moderate δ although two symmetrical about $\delta=0$ local minima are clearly visible. This feature is of importance since the local minimum carries information about the nonlinear anisotropy of the gain medium (i.e., the cross saturation coefficient C_2).

Figures 2(a), 2(b), and 3 demonstrate that there are two qualitatively different ways of changing the laser behavior when one of the two modes (x or y) loses its stability. First, for small $|\Delta|$, $|\delta|$, or large η there are domains in which both

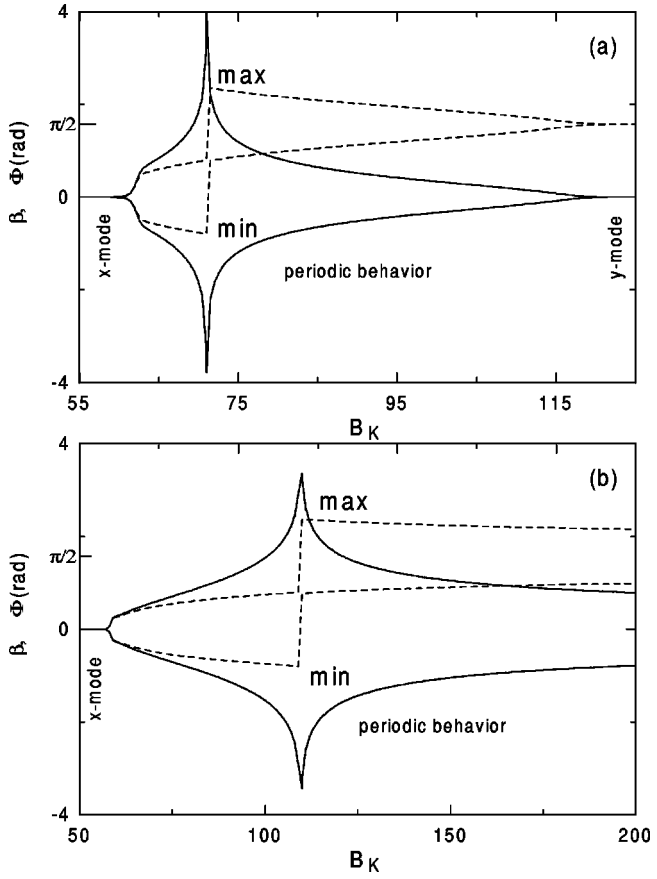

FIG. 4. One parameter diagram of the ellipticity parameter β (continuous lines) and the polarization azimuth (dashed lines) as a function of the nonlinearity parameter B_K for $\delta=0$, $\eta=1.33$, $p=0.999$, and (a) $\Delta=-0.025$ rad and (b) $\Delta=-0.035$ rad. Lower (upper) curves show maxima (minima) of the variables.

modes are stable. Numerical integration of the laser equations shows that in such a case the system always switches to the alternative stable LP mode when one of them undergoes a Hopf bifurcation. The limit cycle attractor emerging at the Hopf bifurcation point becomes immediately unstable. Second, for large $|\Delta|$, $|\delta|$, or small η there are domains in which neither one of the LP modes is stable. For this case destabilization of the stable LP steady-state leads to time-dependent laser output with periodic oscillations of the field intensity and polarization parameters.

Figure 4 illustrates the development of the periodic instabilities, showing the amplitude of the oscillations of the laser field polarization parameters, as the control parameter B_K varies. Figure 4(a) depicts a situation when a limit cycle attractor develops from the Hopf bifurcation of the x mode and vanishes at the Hopf bifurcation of the y mode. In Fig. 4(b) periodic behavior persists until relatively large values of B_K. Note that when the ellipticity parameter tends to its critical magnitudes, $\beta \to \pm\infty$ (recall, this corresponds to the right/left circular polarization), the mean value of the polarization azimuth oscillations changes from 0 to $\pi/2$, but the azimuth remains oscillating. Figure 5 displays phase trajectories of the periodic attractor on the plane (β, Φ) and evolution of the laser polarization state on the Poincaré sphere

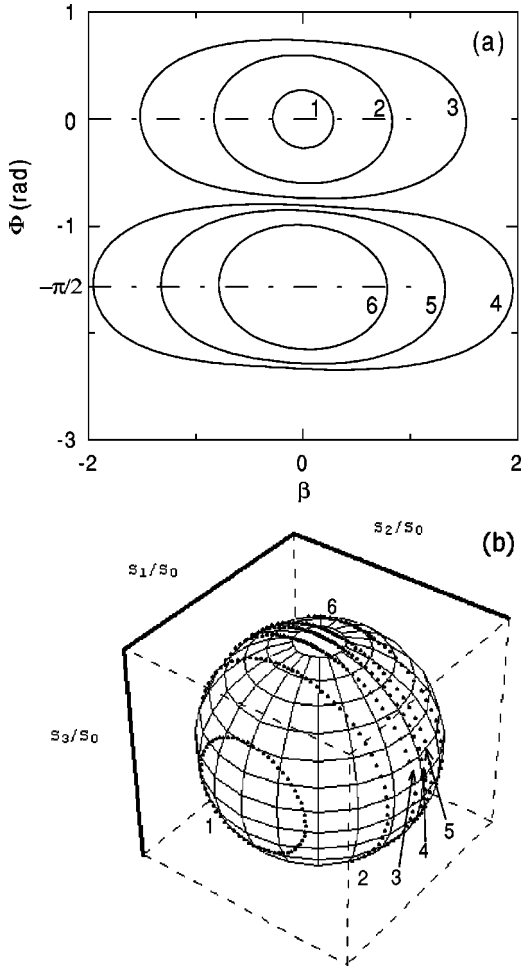

FIG. 5. Phase projections of the limit cycle attractor on the plane (β, Φ) and the trajectory of the laser field polarization state on the Poincaré sphere in the case of Fig. 4(b) and for $B_K=60$ (1), 80 (2), 100 (3), 115 (4), 130 (5), and 200 (6). S_0, S_1, S_2, and S_3 are the Stokes parameters.

for several values of B_K. Clearly, at the Hopf bifurcation point (Fig. 5, curve 1) both polarization parameters behave harmonically, which is a consequence of the critical slowing down near a bifurcation point [19]. Moving away from this bifurcation point phase projections deform, reflecting the influence of the specific physical situation. Trajectories on the Poincaré sphere form concentric circumferences that occupy the west [$-\pi/4<\Phi<\pi/4$, Fig. 5(b), curves 1–3] and the east [$\pi/4<\Phi<-\pi/4$, Fig. 5(b), curves 4–6] hemispheres. Approaching the meridian, which delimits these hemispheres, the polarization azimuth remains nearly constant (at $\pm\pi/4$) as long as the ellipticity angle is not very large and rapidly changes from $\Phi\approx+\pi/4$ ($-\pi/4$) to $-\pi/4$ ($+\pi/4$) when the ellipticity angle tends to the North (South) pole. In contrast to the polarization parameters, the laser field intensity exhibits barely perceptible fluctuations around large mean value. The amplitude of these oscillations does not depend significantly on the control parameters, although the average intensity gradually decreases as B_K increases. Such time-dependent amplitude-polarization behavior of the laser field does not qualitatively change in all the instability domains.

These results clearly show that such vector laser systems can be powerful, accurate, highly sensitive, and inexpensive tools for measurements. Indeed, the field-independent anisotropy of the Kerr material Δ_- (which is induced by the effect of natural optical activity) can be simply measured by registering the turning angle of the polarization plane of the emitted field. Accuracy of these measurements will be limited to the accuracy of the specific laboratory detector. However, since the natural rotatory power of many materials is rather strong (up to thousands grad/cm), the turning angle can be easily measured with rather high precision even with standard detectors. In contrast, the third-order nonlinearities are very small and usually require either an intense optical field and/or long Kerr cells for direct measurements [3,2] or the development of alternative methods [7]. However, because of a third-order process, even with laser sources for the strong optical field there are problems with precision and sensitivity of the measurements. In the proposed method modulus of the third-order nonlinearity $\chi^{(3)}_{1221}$ can be determined by measuring the control parameters at which the Hopf bifurcations of the LP laser modes occur [see (16)]. Since the Hopf bifurcations define eventually the ratio of the Kerr to gain medium nonlinearities (i.e., $\chi^{(3)}_{1221}/\chi^{(3)}_m$), sensitivity of the method is rather high. Roughly, it is of the order of the coefficient $\chi^{(3)}_m l/l'$. Hence, even very weak Kerr nonlinearities (of the order of 10^{-15} esu or less) should be readily measured in an experiment. In addition, because $\chi^{(3)}_m$ ($=\sqrt{\pi}N_m|d_{12}|^4/9\hbar^3 Ku\gamma_1\gamma_2$) can be varied over a wide range by an appropriate choice of the gain mixture or appropriate adjusting gain, pressure of the active medium, length of the gain tube, and so on, sensitivity of the system can be a controllable factor. High precision of the method is ensured by the fact that all measurements can be performed at relatively large cavity anisotropies when the laser system is stable against environmental conditions that often limits intracavity measurements in weakly anisotropic lasers. Moreover, in practice the instability thresholds (and, as a consequence, $\chi^{(3)}_{1221}$) can be found relatively easily in the bistability domain because of sudden switches of the laser emission from one LP mode, which is destabilized at the corresponding Hopf bifurcation point, to the alternative stable orthogonally polarized mode. Clearly, such a polarization flip can be conveniently recognized in an experiment. Precision of the measurements of the bifurcation value of the control parameter in this case will be even better than that registering conventional development of periodic instabilities at a supercritical Hopf bifurcation with smooth variation of the amplitude of the field parameter oscillations. In addition, the *presence* of the instabilities for given phase anisotropy can be a test on the sign of $\chi^{(3)}_{1221}$ since the Hopf bifurcations are not symmetric with respect to the change of sign of Δ. Finally, because this method requires only standard laboratory equipment and a relatively simple experimental setup, all measurements can be done with much less effort than those involving more direct methods [2,3].

It is worth noting also that in spite of the long history of studies of nonlinear dynamics of lasers with or without numerous intracavity complications, the problem discussed in

this work remains practically unexplored while it is interesting both from fundamental and applied points of view. This is due to the fact that only recent theoretical works have clarified the crucial role of polarization (or, more generally, vectorial) degree of freedom in development of laser instabilities [4,6,14,20–22]. In particular, it has been shown that vectorial degrees of freedom are responsible for complex dynamics in single longitudinal-transverse-polarization mode nonautonomous class-A [23] and autonomous class-B [24] vector lasers that was impossible in the scalar case. That is why we believe that our results along with a straightforward experimental arrangement might stimulate experimental investigations of vectorially induced instabilities in laser systems.

IV. ZEEMAN LASER

It is well known that even a weak magnetic field, such as that of the Earth, can significantly modify behavior of vector lasers [6,17,20,25–27]. Here we investigate an effect of the longitudinal magnetic field on the dynamics of our laser nonlinear system. A parameter describing the magnetic field (Δ_B') will be rescaled to the Doppler profile width (Ku) and denoted as $\Delta_B \equiv \Delta_B'/Ku$. The motion equations for this case are given by the complete system (10).

Equations (10) no longer admit LP solutions. Moreover, it is hardly possible to find analytically the laser steady states. A more efficient way in such a case is the numerical integration of the system. Numerical scanning of the parameter subspace (Δ, Δ_B) gives qualitatively different results for small and large Kerr nonlinearity. Figure 6 illustrates a different structure of phase space for $B_K=57$ (small) and $B_K=100$ (large).

Before continuing, let us recall that in a Zeeman laser with no Kerr cell the steady-state solutions are, generally, elliptically polarized (EP). Their helicity is determined by the signs of Δ_B and Δ in such a way that the former x (y) LP mode for negative Δ and positive Δ_B becomes the left (right) EP mode. Changing the sign of Δ to positive, the helicities of both EP solutions interchange [6]. Because for large Δ the ellipticity of these modes is negligible, it is convenient to retain notations x and y for the new EP states. However, they will be used with subscripts L and R to refer to their helicity. For example, for $\Delta_B>0$ and $\Delta<0$ the former x (y) mode corresponding to Fig. 2 becomes a left- (right-) handed EP mode with close to 0 ($\pi/2$) azimuth, i.e., x_L (y_R) mode. Consequently, for $\Delta_B>0$ and $\Delta>0$ one has x_R and y_L modes.

For small B_K [Fig. 6(a)] two qualitatively different types of laser behavior are distinguished. For small $|\Delta|$ time-dependent dynamics is mainly governed by the applied magnetic field [6]. An impact of the nonlinearity B_K onto this behavior is the asymmetry of the instability domain M confined by the Hopf bifurcations B_M^{xL} and B_M^{xR}, which destabilize the x_L and x_R modes, respectively (they are not present in the case of the laser with no magnetic field). Instabilities attributed to the Kerr nonlinearity (domain K) and the bistable behavior of the x_L and y_R modes constitute an alternative type of the laser behavior. In contrast to the first type,

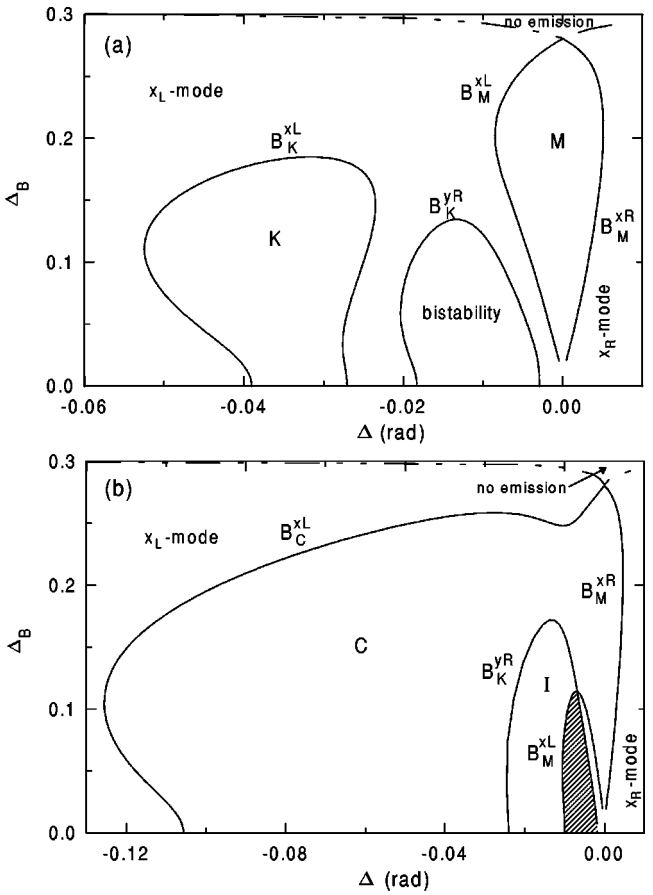

FIG. 6. The Hopf bifurcations of the steady states of the Zeeman laser are depicted in the subspace (Δ, Δ_B) for $\eta=1.33$, $\delta=0$, $p=0.999$, and (a) $B_K=57$ and (b) $B_K=100$. The remaining parameters correspond to Fig. 2. For other notations, see the text.

this behavior is more sensitive to the change of Δ_B. At first, an increase of Δ_B results in the progressive enlarging instability domain K. However, thereafter the bistability and instability K domains diminish and totally vanish through inverse Hopf bifurcations B_K^{yR} and B_K^{xL} for $\Delta_B \gtrsim 0.13Ku$ and $\Delta_B \gtrsim 0.18Ku$, respectively. Outside the instability domains and to the left (right) of the boundary B_M^{xL} (B_M^{xR}), the stable solution for $\Delta_B>0$ is the x_L (x_R) mode. Thus, the y_R mode is stable only inside the bistability domain while the y_L mode is never stable for $\Delta_B>0$ and such a relatively large amplitude anisotropy ($p=0.999$). Figure 6(b) shows that for large B_K instability domains associated with the effects of the magnetic field and the Kerr nonlinearity collide producing combined instability domain C. From the ''above'' this domain is confined by the Hopf bifurcation of the x_L mode (B_C^{xL}). In domain I the y_R mode is stabilized by the Hopf bifurcation B_K^{yR}. The bistability domain of the x_L and y_R modes distinguished by the Hopf bifurcations B_K^{yR} and B_M^{xL} is hatched. Again, there are neither bistability nor instabilities to the right of the boundary B_M^{xR}, where the laser operates on the x_R mode. Note that for small Δ and Δ_B the Hopf bifurcations turn to be saddle-node bifurcations as discussed in [6] (they are not shown in Fig. 6).

For the sake of illustration, the behavior of the laser field

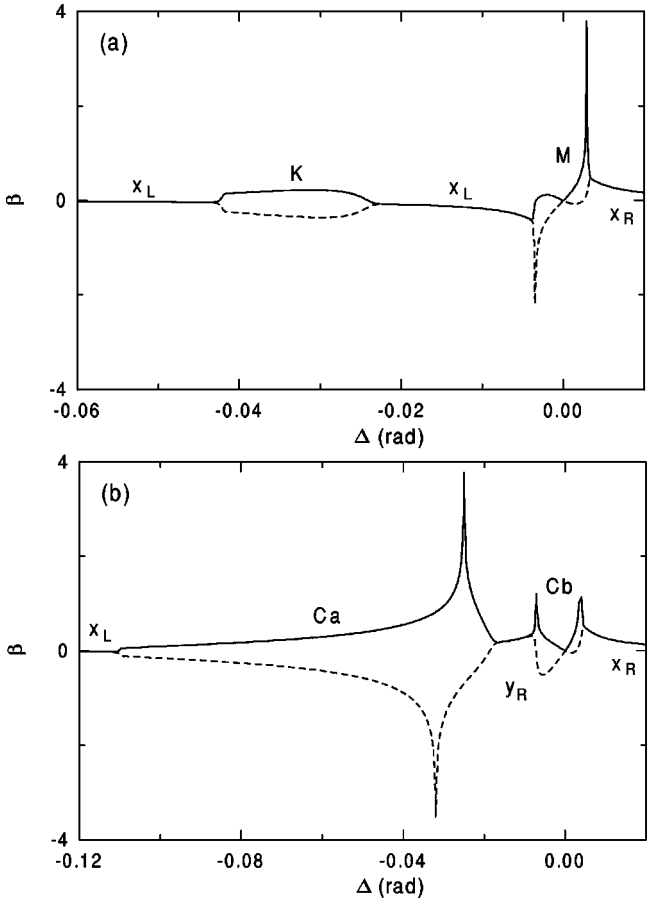

FIG. 7. One parameter diagram of the ellipticity angle β as a function of the phase anisotropy for $B_K=57$, $\Delta_B=0.1$ (a) and $B_K=100$, $\Delta_B=0.15$ (b). The other parameters are the same as in Fig. 6. Continuous (dashed) lines show maxima (minima) of β. For other notations, see the text.

ellipticity corresponding to Figs. 6(a) and 6(b) for $\Delta_B=0.1$ and $\Delta_B=0.15$ is depicted in Figs. 7(a) and 7(b), respectively. Figure 7(a) clearly shows that dynamics in the instability domains *M* and *K* is qualitatively different. While in domain *K* one observes a small amplitude weakly dependent on Δ oscillations, in domain *M* the amplitude of the ellipticity oscillations changes significantly. The behavior of the polarization azimuth in domain *K* is qualitatively similar to that of the ellipticity. However, in domain *M* the azimuth shows oscillating behavior only at the domain edges. In between the two large spikes, i.e., when the ellipticity angle β tends to infinity, the azimuth turns out to be continuously rotating instead of oscillating. The latter feature is a characteristic feature of Zeeman lasers (compare with Fig. 4 in which polarization azimuth remains oscillating in spite of the fact that β undergoes the extreme values).

For large B_K [Fig. 7(b)] periodic behavior of the polarization parameters in the instability domains Ca and Cb is more pronounced. One can see that for moderate $|\Delta|$, a minimum of the ellipticity oscillations goes to $-\infty$. This is the point where polarization azimuth oscillations (around a mean value close to 0) become a continuous rotation, which is directly attributed to the influence of the magnetic field. At another extreme value ($\beta\rightarrow+\infty$), the azimuth rotation again becomes periodic oscillations but now it oscillates around the mean value which is close to $\pi/2$. Similar behavior with rotating azimuth occurs in domain Cb. Ellipticity of the field in the instability domains evolves periodically in time in accordance with the sequence: right EP $\rightarrow$ LP $\rightarrow$ left EP $\rightarrow$ LP $\rightarrow\cdots$, and so on. In between the domains Ca and Cb laser emission is stable. The y_R mode in this domain is stabilized by the B_K^{yR} Hopf bifurcation.

V. CONCLUSIONS

We have presented the results of analytical and numerical studies of nonlinear dynamics of a class-*A* Fabry-Pérot weakly anisotropic laser containing a Kerr cell filled with an anisotropic third-order nonlinear material. Field-independent anisotropy of the Kerr material was induced by the effect of natural optical activity. Anisotropy of the bare laser cavity was assumed to be linear (i.e., in the Cartesian basis) since this was the case for many realistic weakly anisotropic lasers. As a specific but rather general example, a typical commercially available He-Ne laser operating at $\lambda=1.15$ μm ($j=1\rightarrow j'=2$) has been considered in all numerical illustrations.

It is shown that such a nonlinear system can exhibit periodic amplitude-polarization instabilities of a single longitudinal-transverse-polarization pattern. These instabilities, which are readily accessible experimentally, are attributed to the vectorial degree of freedom and they are not allowed when the field polarization state is fixed. More important is that the vectorial degree of freedom results in a qualitatively new phase in elaboration of inverse methods of measurements. Specifically, the whole complex of static and dynamical phenomena displayed by this system gives rise to a comprehensive, inexpensive, highly sensitive, and effective method of measurement of material anisotropies. Moreover, static and dynamical features of the system naturally separate contributions of the field-independent and nonlinear anisotropies.

In particular, it is found that basic steady states of this vector nonlinear laser system are orthogonal modes, which are linearly polarized (LP) in the Cartesian basis. Under stationary laser operation, anisotropies of the Kerr material affect the only parameter of the laser field, i.e., the field polarization azimuth. Half of the turning angle of the polarization plane of the emitted laser field provides the magnitude of the field-independent anisotropy of the Kerr material. Direction of the polarization plane rotation gives sign of this anisotropy. Although the Kerr nonlinearity has no effect on the LP laser steady states, an impressive feature of this system is that it does affect the *stability* of these modes and, as a consequence, the laser time-dependent behavior. The onset of the instabilities (i.e., the Hopf bifurcation) in the system defines the ratio $\chi^{(3)}_{1221}l'/\chi^{(3)}_{m}l$. Obviously, this fact can be employed for measurements of the nonlinear anisotropy of the matter. Moreover, because the Hopf bifurcations are proportional to the *ratio* of the material nonlinearities, such a method might be very sensitive because nonlinear processes in the gain and Kerr media are of the same third order. The

presence of the instabilities for a given laser cavity phase anisotropy is a test on the sign of $\chi^{(3)}_{1221}$.

From the experimental point of view, the system investigated admits an easy registration of the instability thresholds for the x and y modes (and, consequently, parameter $\chi^{(3)}_{1221}$) because the laser cavity anisotropy should not be too weak for that. Furthermore, high accuracy of the method can even be enhanced by the bistability phenomenon: when the laser mode loses its stability in the bistability domain, the laser emission is found to suddenly switch to the alternative stable LP mode. Such a polarization flip can be easily revealed in an experiment and measured with high precision. Indeed, if the laser output field propagates through a polarizer aligned with the field polarization plane, the loss of the stability of this mode will result in the total disappearance of the laser emission after the polarizer. No doubt, registration of this behavior can be easily performed even in an automatic manner. Finally, because this method requires only standard laboratory equipment and straightforward experimental arrangement, all measurements can be done with much less effort than in the case of employing direct methods of measurement.

The effects of the cavity amplitude and phase anisotropy, laser field detuning, and gain on the behavior of the Hopf bifurcations is studied in detail. The main conclusion is that large gain, amplitude anisotropy, and detuning and excessively small and large cavity phase anisotropy decrease the laser sensitivity to the Kerr nonlinearity. We have also investigated dynamics of this laser system subject to the action of a longitudinal magnetic field. Because the Kerr nonlinearity is more efficient at relatively large and moderate $|\Delta|$, its effect on the laser dynamics can be readily set apart from that of the magnetic field when B_K, is small. For large $|B_K|$, the laser time-dependent behavior is a combined response of the system to the effects of the Kerr nonlinearity and the magnetic field.

[1] Y. I. Khanin, *Principles of Laser Dynamics* (Elsevier, Amsterdam, 1995).

[2] Y. R. Shen, *The Principles of Nonlinear Optics* (John Wiley & Sons, New York, 1984).

[3] Yu. P. Svirko and N. I. Zheludev, *Polarization of Light in Nonlinear Optics* (John Wiley & Sons, Chichester, 1998).

[4] See, for instance, Quantum Semiclassic. Opt. **10** (1) (1998), special issue on polarization effects in lasers and spectroscopy, edited by N. B. Abraham and G. M. Stephan.

[5] C. O. Weiss and R. Vilaseca, *Dynamics of Lasers* (VCH, Weinheim, 1991).

[6] A. Kul'minskii, Yu. Loiko, and A. Voitovich, Opt. Commun. **167**, 235 (1999).

[7] S. C. Read, A. D. May, and G. D. Sheldon, Can. J. Phys. **75**, 211 (1997).

[8] A. Voitovich and V. Severikov, *Lasery s Anisotropnymi Resonatorami* (*Anisotropic Cavity Lasers*) (Nauka i Tekhnika, Minsk, 1988), in Russian.

[9] A. Voitovich, A. Kul'minskii, and V. Severikov, Opt. Commun. **126**, 152 (1996).

[10] A. D. May, and G. Stephan, J. Opt. Soc. Am. B **6**, 2355 (1989); P. Paddon, E. Sjerve, A. D. May, M. Bourouis, and G. Stephan, *ibid.* **9**, 574 (1992).

[11] K. Ait-Ameur, G. Stephan, P. Paddon, and A. D. May, Appl. Opt. **33**, 334 (1994).

[12] M. Haelterman and M. D. Tolley, Opt. Commun. **108**, 165 (1994).

[13] V. A. Makarov, and A. V. Matveeva, Kvant. Elektron. (Moscow) **15**, 138 (1988) [Sov. J. Quantum Electron. **18**, 89 (1988)].

[14] A. Kul'minskii, V. Severikov, and A. Voitovich, Quantum Semiclassic. Opt. **10**, 107 (1998).

[15] N. Bloembergen, *Nonlinear Optics* (Benjamin, New York, 1965).

[16] R. Loudon, *The Quantum Theory of Light* (Clarendon Press, Oxford, 1973).

[17] A. Voitovich, A. Kul'minskii, Yu. Loiko, and V. Severikov, Izv. Akad. Nauk Ross., Ser. Fiz. **60**, 110 (1996) [Bull. Russ. Acad. Sci., **60**, 421 (1996)].

[18] I. I. Savel'ev, A. M. Khromykh, and A. I. Yakyshev, Kvant. Elektron. (Moscow) **6**, 1155 (1979) [Sov. J. Quantum Electron. **9**, 682 (1979)].

[19] P. Mandel, *Theoretical Problems in Cavity Nonlinear Optics* (Cambridge University Press, Cambridge, 1997).

[20] A. D. May, P. Paddon, E. Sjerve, and G. Stephan, Phys. Rev. A **53**, 2829 (1996).

[21] L. Gil, Phys. Rev. Lett. **70**, 162 (1993); M. San Miguel, *ibid.* **75**, 425 (1995).

[22] N. B. Abraham, M. D. Matlin, and R. S. Gioggia, Phys. Rev. A **53**, 3514 (1996); M. D. Matlin, R. S. Gioggia, N. B. Abraham, P. Glorieux, and T. Crawford, Opt. Commun. **120**, 204 (1995); N. B. Abraham, E. Arimondo, and M. San Miguel, *ibid.* **117**, 344 (1995).

[23] A. Kul'minskii, V. Severikov, and A. Voitovich, J. Opt. B: Quantum Semiclass. Opt. **1**, 294 (1999).

[24] J. Martin-Regalado, F. Prati, M. San Miguel, and N. B. Abraham, IEEE J. Quantum Electron. **33**, 765 (1997); M. Travagnin, M. P. van Exter, A. K. Jansen van Doorn, and J. P. Woerdman, Phys. Rev. A **54**, 1647 (1996); A. Voitovich, A. Kul'minskii, and Yu. Loiko, Dokl. Nat. Acad. Sci. Belarus **43**, 52 (1999).

[25] J. Cotteverte, F. Bretenaker, and A. Le Floch, Opt. Commun. **79**, 152 (1996).

[26] A. Voitovich, L. Svirina, and V. Severikov, Opt. Commun. **80**, 435 (1991).

[27] E. Sjerve, Ph.D. thesis, University of Toronto, 1995; P. Paddon, Ph.D. thesis, University of Toronto, 1995.